Strojniški vestnik - Journal of Mechanical Engineering 57(2011)12, 911-926
DOI: 10.5545/sv-jme.2011.100
Paper received: 15.03.2011
Paper accepted: 28.07.2011

Simulation of Water-Gas Shift Membrane Reactor for Integrated Gasification Combined Cycle Plant with CO_2 Capture

Andrej Lotrič[1,*] – Mihael Sekavčnik[1] – Christian Kunze[2] – Hartmut Spliethoff[2]
[1]University of Ljubljana, Faculty of Mechanical Engineering, Slovenia
[2]Technische Universität München, Institute for Energy Systems, Germany

The effectiveness of energy conversion and carbon dioxide sequestration in Integrated Gasification Combined Cycle (IGCC) is highly dependent on the syngas composition and its further processing. Water gas shift membrane reactor (WGSMR) enables a promising way of syngas-to-hydrogen conversion with favourable carbon dioxide sequestration capabilities. This paper deals with a numerical approach to the modelling of a water gas shift reaction (WGSR) in a membrane reactor which promotes a reaction process by selectively removing hydrogen from the reaction zone through the membrane, making the reaction equilibrium shifting to the product side. Modelling of the WGSR kinetics was based on Bradford mechanism which was used to develop a code within Mathematica programming language to simulate the chemical reactions. The results were implemented as initial and boundary conditions for the tubular WGSMR model designed with Aspen Plus software to analyze the broader system behaviour. On the basis of selected boundary conditions the designed base case model predicts that 89.1% CO conversion can be achieved. Calculations show that more than 70% of carbon monoxide conversion into hydrogen appears along the first 40% of reactor length scale. For isothermal conditions more than two thirds of the heat released by WGSR should be extracted from the first 20% of the reactor length. Sensitivity analysis of the WGSMR was also performed by changing the membrane's permeance and surface area.

Keywords: IGCC, water-gas shift reaction, membrane reactor

0 INTRODUCTION

Gasification is an exothermal chemical process at high temperatures and pressures between a hydro-carbonaceous material and an oxidizer (air, oxygen and/or steam). In general, the feedstock used for gasification consists of hydrocarbons and can be in different forms like coal, oil, heavy refinery residuals, coke, biomass or even municipal waste. As the oxygen supply is limited (generally 20 to 70% of the oxygen needed for complete combustion) only partial combustion of the feedstock occurs. The released heat from the chemical reaction drives the secondary reaction that further converts organic material to syngas.

Syngas is mostly a mixture of CO, H_2, CO_2 and some CH_4, H_2O and N_2. The ratio between CO, H_2 and CO_2 can be quite different as it depends on the type of a gasifier (moving-bed, fluid-bed or entrained-flow gasifier) and the gasifying feedstock. To achieve the desired composition of syngas the correct operating temperature – hence the correct amount of oxidizer for partial combustion – and pressure of gasification must be selected.

The operating temperature can range between 800 and 1800 °C and the pressure between 10 and 100 bar.

Gasification is one of the main processes in integrated gasification combined cycle (IGCC) energy systems. In general, all existing IGCC power plants follow the chain of events presented in Fig. 1 with an exception of carbon dioxide sequestration (CCS). This chain can be broken down into ten key processes [1]:

1. Air separation unit (ASU) separates air into oxygen to supply the gasifier and nitrogen, which can be used as a carrier, sweep or dilution gas.
2. Coal particles are transferred – using pneumatic conveying or in a form of water-coal slurry – into a gasifier.
3. By-products captured in the gasifier (ash and slag) can have commercial value, depending on local market conditions.

*Corr. Author's Address: University of Ljubljana, Faculty of Mechanical Engineering, Laboratory for Heat and Power, Aškerčeva 6, 1000 Ljubljana, Slovenia, andrej.lotric@gmail.com

4. The syngas also has small amounts of other impurities (e.g. H_2S, COS, NH_3 and also chlorides, fluorides, mercury etc.) which are removed during the gas clean-up. Before the clean-up process syngas is cooled, usually in a syngas cooler, where part (or all) of the steam used in the gasification process is produced.
5. Around 99% of H_2S is separated from the syngas and converted to elemental sulphur or possibly sulphuric acid.
6. Nowadays, the syngas is passed through a two stage WGS reactor and reacted over a catalyst with added steam to convert the majority of the CO into CO_2 and additional H_2. The H_2 is separated from the gas mixture usually by using the pressure swing adsorption (PSA) process.
7. The future potential of IGCC systems is the CO_2 removal, leaving H_2-rich syngas behind.
8. Syngas can also be used in variety of processes; like production of synthetic fuels or chemicals and pure H_2 can be used in fuel cells or combined cycle to produce electricity.
9. The main cause for IGCC plants being more efficient than conventional power plants is the combined use of a gas and a steam turbine to produce electricity.
10. Much of the water used in this process is recycled in the plant, while some is evaporated in a cooling tower.

1 WATER-GAS SHIFT REACTION PROCESS

1.1 Membrane Reactor

In general, the membrane reactor (MR) is a device that combines a membrane separation process with a chemical reactor in one unit. The MR is capable of promoting a reaction process by selectively removing at least one of the products from the reaction zone through the membrane, making the equilibrium reaction shifting to the product side.

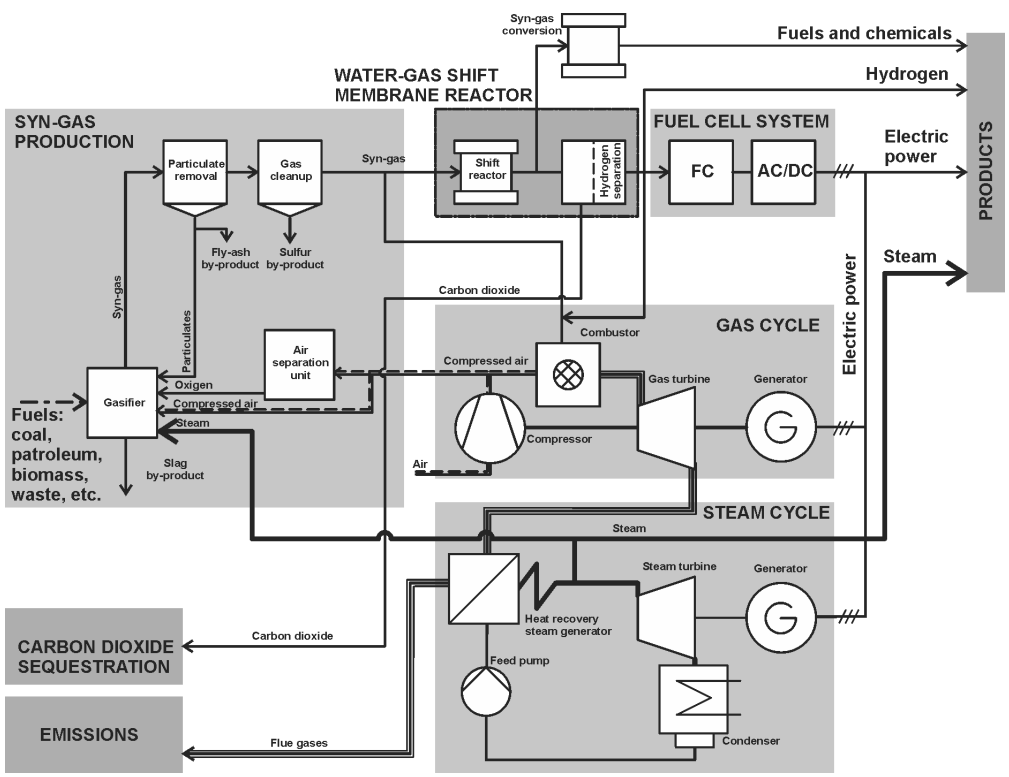

Fig. 1. *Schematic presentation of the syngas production, hydrogen separation, CCS and hydrogen utilisation in the IGCC*

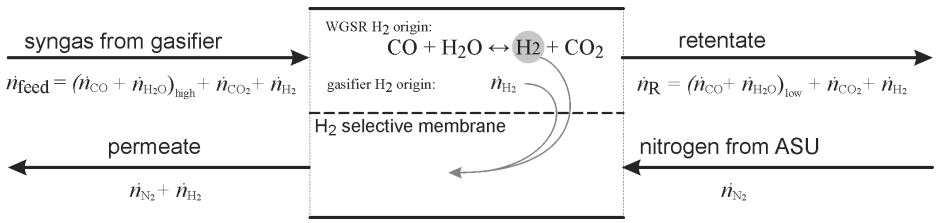

Fig. 2. *WGSR process in the MR*

The membrane used is highly selective to the product of interest therefore, the product can be directly recovered during the reaction, eliminating the need for additional product purification steps.

The rate of the product flux through the membrane is proportional to the product's partial pressure difference between the process (feed) side and the permeate side; therefore, the extracted product is recovered at a lower pressure than the process stream pressure. To increase the pressure difference, the inert diluting (or carrier) gas is sometimes used. The diluting gas is carrying away the permeated product therefore, reducing the concentration on the permeate side and thus, increasing the driving force for permeation. The pressure drop through the membrane is material dependent, and it obeys different laws for different membrane materials.

With MR the yield can be increased (even beyond the equilibrium value for equilibrium reactions) and/or the selectivity can be improved by suppressing other undesired side reactions or the secondary reaction of products. Due to the integration of reaction and separation, chemical processes become simpler leading to a much lower processing cost.

1.2 Water-Gas Shift Reaction

The equilibrium of reversible reactions can be shifted toward more product formation by changing reaction conditions such as pressure and temperature or concentrations of reactants or products.

The main focus of this paper is the Water-Gas Shift Reaction (WGSR), which is also an equilibrium reaction and it is represented with the following equation:

$$CO + H_2O \leftrightarrow CO_2 + H_2 - 41 \text{ MJ/kmol} . \quad (1)$$

According to Eq. (1) changing the pressure of the WGSR should not have any considerable effect on changing the equilibrium concentrations because the equation is equimolar. However, the experimental results, obtained from [2], show that very high pressures slightly favour the CO conversion which can be seen in the Table 1.

Table 1. *Effect of pressure on equilibrium CO concentrations (inlet dry gas: 13.2% CO, 10.3% CO_2, 35.3% H_2, 41.2% N_2, steam-to-dry gas = 0.5)*

Tempe-rature [°C]	p = 3.04 bar [% CO]	p = 30.39 bar [% CO]	p = 303.9 bar [%CO]
200	0.12	0.12	0.07
300	0.68	0.65	0.48
400	1.98	1.94	1.61
500	3.93	3.88	3.46
600	6.15	6.10	5.68
700	8.38	8.34	7.95

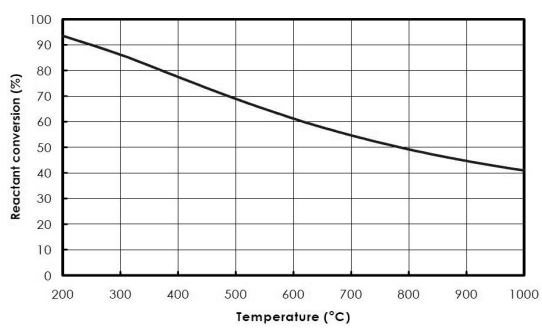

Fig. 3. *Reactant conversion for the WGSR where H_2 and CO_2 are not present at the beginning [3]*

On the other hand, it is well known that increasing the temperature has a decreasing effect on equilibrium CO conversion. Therefore, H_2 yield can be considerably enhanced at high

reaction temperatures, at which the equilibrium CO conversion would otherwise be low, by extracting either CO_2 or H_2 from the reaction mixture.

1.3 Water-Gas Shift Kinetics

1.3.1 General Definition of Rate Law

Chemical kinetics investigates how different experimental conditions can influence the chemical reaction rate. The main factors that can speed up the reaction rate include increase in the concentrations of the reactants, increase in temperature or pressure at which the reaction occurs and whether or not any catalysts are present in the reaction.

Usually, what appears to be a single step conversion is in fact a multistep reaction and thus, the reaction mechanism is a step by step sequence of elementary reactions. Each step has its own rate law and molecularity (the number of species taking part in that step); therefore the slowest step is the one that determines the overall reaction rate – the rate limiting step.

Only for simple (elementary) reactions a partial order of reaction is the same as the stoichiometric number of the reactant concerned. For stepwise reactions there is no general connection between stoichiometric numbers and partial orders. Such reactions may have more complex rate laws and the orders of reaction are in principle always assigned to the elementary steps.

By conducting experiments involving reactants A and B, one would find that the rate of the reaction r is related to the concentrations *[A]* and *[B]* in a rate law as:

$$r = k\,[A]^a\,[B]^b\,, \tag{2}$$

where k is the rate constant and the powers a and b are called the partial orders of the reaction. The overall order of the reaction is found by adding up the partial orders. The rate constant is not a true constant because it is dependent on the reaction's temperature T and the activation energy E_a and is defined via Arrhenius equation as:

$$k = k_0 \cdot e^{-\frac{Ea}{R \cdot T}}, \tag{3}$$

where k_0 is the pre-exponential factor.

A pair of forward and backward reactions may define an equilibrium process where A and B react into C and D and vice versa (a, b, c and d are the stoichiometric coefficients):

$$a\,A + b\,B \Leftrightarrow c\,C + d\,D \tag{4}$$

Assuming that above reactions are elementary, the reaction rate can be expressed as:

$$r = k_1 \cdot [A]^a \cdot [B]^b - k_2 \cdot [C]^c \cdot [D]^d\,, \tag{5}$$

where k_1 is the rate coefficient for the forward reaction which consumes A and B; k_2 is the rate coefficient for the backward reaction, which consumes C and D.

In a reversible reaction, like WGSR, chemical equilibrium is reached when the rates of the forward and backward reactions are equal and the concentrations of the reactants and products no longer change ($r = 0$ in balance).

1.3.2 Bradford Mechanism

a) Backward WGSR

Bradford [4] assumed that the reaction mechanism would follow the simple gas-phase chain-reaction mechanism given below (M indicates any gas-phase collision partner). The chain is initiated by the gas-phase dissociation of hydrogen (Eq. (6)). Propagation steps are represented by reactions in Eqs. (7) and (8). The termination step corresponds to the gas-phase re-association of H_2 in Eq. (9), consuming the chain carriers.

$$\mathrm{H_2} + M \xrightarrow{k_1} 2\mathrm{H} + M, \tag{6}$$

$$\mathrm{H} + \mathrm{CO_2} \underset{k_{-2}}{\xleftarrow{\qquad}} \xrightarrow{k_2} \mathrm{CO} + \mathrm{OH}, \tag{7}$$

$$\mathrm{OH} + \mathrm{H_2} \underset{k_{-3}}{\xleftarrow{\qquad}} \xrightarrow{k_3} \mathrm{H_2O} + \mathrm{H}, \tag{8}$$

$$2\mathrm{H} + M \xrightarrow{k_{-1}} \mathrm{H_2} + M. \tag{9}$$

With the assumption of low conversion and a stationary state for the concentrations of the intermediates (H and OH concentrations do not change significantly with respect to time), the following rate equation r_b is obtained,

$$r_b = \frac{d[\mathrm{CO}]}{dt} = \left(\frac{k_1}{k_{-1}}\right)^{1/2} \cdot k_2 \cdot [\mathrm{H_2}]^{1/2} \cdot [\mathrm{CO_2}]. \tag{10}$$

Therefore, the rate constant for the backward WGSR k_b may be expressed as:

$$k_b = \left(\frac{k_1}{k_{-1}}\right)^{1/2} \cdot k_2, \tag{11}$$

where the temperature dependence of the rate constant is described with the Arrhenius Eq. (3).

Consequently, the expression for the rate of reaction in terms of k_b becomes:

$$r_b = \frac{d[\mathrm{CO}]}{dt} = k_b \cdot [\mathrm{H_2}]^{1/2} \cdot [\mathrm{CO_2}]. \tag{12}$$

b) Forward WGSR

The gas-phase, chain-reaction mechanism proposed by Bradford [4] can also be used to describe the forward WGSR. Reaction in Eq. (13) provides the chain initiation by the reaction of H_2O with any gas-phase molecule (designated by M). Reactions in Eqs. (14) and (15) are the propagation steps, while the reaction in Eq. (16) is the termination step.

$$\mathrm{H_2O} + M \xrightarrow{k_4} \mathrm{H} + \mathrm{OH} + M, \tag{13}$$

$$\mathrm{CO} + \mathrm{OH} \underset{k_{-5}}{\xleftarrow{\qquad}} \xrightarrow{k_5} \mathrm{H} + \mathrm{CO_2}, \tag{14}$$

$$\mathrm{H_2O} + \mathrm{H} \underset{k_{-6}}{\xleftarrow{\qquad}} \xrightarrow{k_6} \mathrm{OH} + \mathrm{H_2}, \tag{15}$$

$$\mathrm{H} + \mathrm{OH} + M \xrightarrow{k_{-4}} \mathrm{H_2O} + M. \tag{16}$$

The stationary-state approximation for the concentration of the chain-carriers (H and OH) under the conditions of low conversions leads to the following expression for the forward WGSR rate of reaction r_f:

$$r_f = \frac{d[\mathrm{CO_2}]}{dt} = \\ = \left(\frac{k_4}{k_{-4}} \cdot k_5 \cdot k_6\right)^{1/2} \cdot [\mathrm{CO}]^{1/2} \cdot [\mathrm{H_2O}]. \tag{17}$$

The rate constant for the forward WGSR k_f is defined as:

$$k_f = \left(\frac{k_4}{k_{-4}} \cdot k_5 \cdot k_6\right)^{1/2}, \tag{18}$$

and the rate can be expressed as:

$$r_f = \frac{d[\mathrm{CO_2}]}{dt} = k_f \cdot [\mathrm{CO}]^{1/2} \cdot [\mathrm{H_2O}]. \tag{19}$$

2 MODEL OF WATER-GAS SHIFT MEMBRANE REACTOR

At the beginning it was assumed that the use of different unit models integrated in simulation software Aspen Plus will be sufficient to model the MR. However, it turned out that the model could not correctly predict the process taking place inside of the reactor. This is why the decision was made to include the WGSR kinetics, which gave a better overview of what occurs inside the reactor.

The modelling of the WGSMR was conducted by using both the Mathematica programming language and Aspen Plus. The calculations made in Mathematica were based on WGSR kinetics and used to predict the reaction

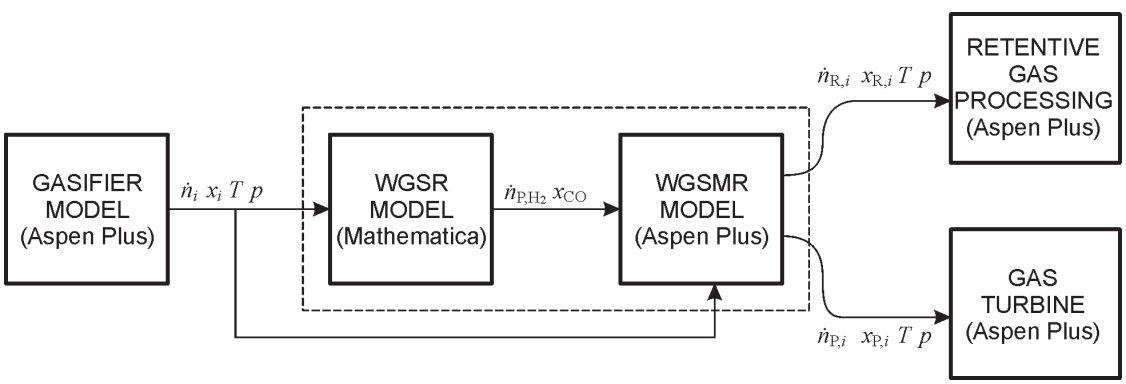

Fig. 4. *Boundary conditions for the modelled system and link between Mathematica and Aspen Plus environment*

rate and the permeation through the membrane. The calculated data were then imported in Aspen Plus as input (or initial) values for simulations.

Aspen Plus was used to predict the behaviour of a WGSMR by using basic engineering relationships, such as mass and energy balances, and phase and chemical equilibrium. According to the calculated data from Mathematica, predicted operating conditions, and different design models, the behaviour of MR was simulated.

2.1 Initial and Boundary Conditions

In IGCC system the MR will be situated after the gasifier and before the gas turbine combustor, replacing the WGS reactor and PSA system (see Fig. 1).

The boundaries for the modelled system are marked with the dashed line in Fig. 4. In this figure $\dot{n}$ represents the molar flow, x the composition, T the temperature and p the pressure of gas stream. Heat duty is represented with $\dot{Q}$ and CO conversion with X_{CO}. Index $_{GAS}$ stands for syngas, $_R$ for retentate side and $_P$ for permeate side of the membrane.

Based on the position in the chain of processes that take part in the IGCC, the initial and boundary conditions for "base case" studies were defined:

a) Based on gasifier:
- The modelling is based on a dry-feed entrained-flow gasifier with water quench. Therefore, the maximum outlet pressure from the gasifier is presumed to be around 50 bar.
- The outlet temperature from the gasifier is set to 1500 °C.
- Composition of syngas has a major role in defining the steam-to-CO ratio and especially in defining the H_2 partial pressure.

b) Based on quench:
- The quench temperature is set to 800 °C. In order to reach this temperature the syngas has to be quenched with water and not steam.
- With pressure of 50 bar, equal to syngas, quench water can only reach temperatures up to 264 °C, otherwise it would begin to vaporise.
- Steam-to-CO ratio is also dependent on the temperature of quench water. Maximum ratio around 1.1 can be reached with quench water at 260 °C.

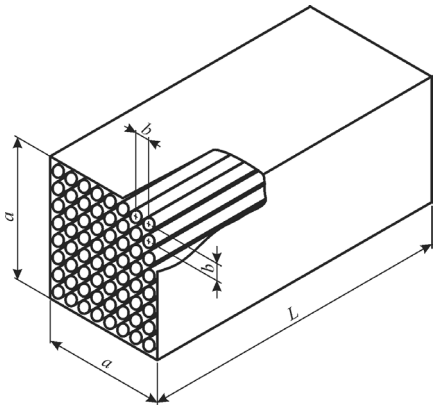

Fig. 5. *Schematic presentation of the reactor model*

c) Based on MR:
- For modelling the tubular MR with gauge measurements L = 40 m and a = 10 m was selected (see Fig. 5). The outer tubular membrane diameter was set to the value $2r$ = 7.5 cm.
- The operational temperature range of the MR is presumed to be between 700 and 900 °C.
- The pressure on the retentate side is defined by the outlet from the gasifier. In this study it is presumed to be 50 bar.
- Low pressure on the permeate side increases the driving force through the membrane. However, from the point of energy loss needed for compression the minimum pressure should not be less than 1 bar.
- In order to improve the driving force the N_2 sweep gas is introduced. In view of syngas the flow of N_2 is in counter-current direction where H_2-to-N_2 molar ratio at the exit is 1:1.
- Since the WGSR is an exothermal reaction, the reactor is water cooled. In the present study the MR will operate at isothermal conditions.
- The desired CO conversion is set to be around 95%.
- Based on the temperature range, pressure conditions, hydrogen purity and permeability, the selected membrane material is Palladium based with permeance: $k' = 3 \cdot 10^{-4}$ mol m^{-2} s^{-1} Pa$^{-0.5}$.

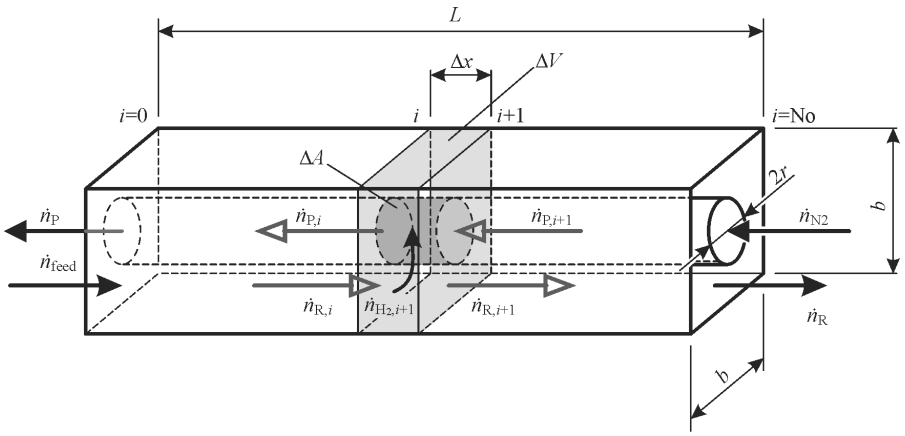

Fig. 6. *Presentation of the numerical model for calculations of WGSR kinetics*

- Due to the high temperatures no catalyst is used for the WGSR.
- In this model it is presumed that the membrane material can withstand the acid environment therefore no pre-cleaning of syngas is needed.
- The model of the reactor is based on a plug flow reactor. This means that there is no change in concentration in radial direction.
- In the kinetic model it is presumed that there are no pressure losses on the retentate or on the permeate side.

2.2 Numerical Model

The numerical model in Mathematica was created in such a way that each reactor tube was divided in N_O = 10,000 infinitesimal sections with length Δx. The calculation started with values obtained from initial and boundary conditions, which gave the values for the first section. In general, the calculations were conducted in such a way that the results from section marked with index i were used to calculate the values indexed as $i+1$ until reaching the last N_Oth section.

a) Retentate side:

Combining Eqs. (5), (12) and (19) the reaction rate for section i+1 was calculated as:

$$r_{i+1} = k_f \cdot [\mathrm{CO}]_i^{1/2} \cdot [\mathrm{H_2O}] - k_b \cdot [\mathrm{H_2}]_i^{1/2} \cdot [\mathrm{CO_2}]_i. \quad (20)$$

The flux in section i+1 was calculated with the following Eq.:

$$J_{i+1} = k' \cdot (\sqrt{p_{RH2,i}} - \sqrt{p_{PH2,i}}), \quad (21)$$

where permeance was held at constant value k' = 3·10^{-4} mol m^{-2} s^{-1} Pa$^{-0.5}$.. This value was selected based on the experimental study made by Ciocco et al. [5] where the permeance of pure Pd membrane k' = 3·10^{-4} mol m^{-2} s^{-1} Pa$^{-0.5}$. was achieved.

Based on Fig. 6 the Law of Conservation of Mass must apply for each section therefore, the molar flow of each specie was calculated with the following set of Eqs.:

$$\dot{n}_{RH2,i+1} = \dot{n}_{RH2,i} + \dot{n}_{reaction,i+1} - \dot{n}_{H2,i+1}, \quad (22)$$

$$\dot{n}_{CO2,i+1} = \dot{n}_{CO2,i} + \dot{n}_{reaction,i+1}, \quad (23)$$

$$\dot{n}_{CO,i+1} = \dot{n}_{CO,i} - \dot{n}_{reaction,i+1}, \quad (24)$$

$$\dot{n}_{H2O,i+1} = \dot{n}_{H2O,i} - \dot{n}_{reaction,i+1}. \quad (25)$$

In the above set of Eqs. $\dot{n}_{reaction,i+1}$ and $\dot{n}_{H2,i+1}$ were defined as:

$$\dot{n}_{reaction,i+1} = r_{i+1} \cdot N_{TUBES} \cdot \Delta V, \quad (26)$$

$$\dot{n}_{H2,i+1} = J_{i+1} \cdot N_{TUBES} \cdot \Delta A. \quad (27)$$

The molar flow of the retentate gas stream was a sum of all calculated molar flows and the inert species in this study (Ar, H_2S, N_2, COS, HCl, CH_4 and others):

$$\dot{n}_{R,i+1} = \dot{n}_{RH2,i+1} + \dot{n}_{CO2,i+1} + \dot{n}_{CO,i+1} + \dot{n}_{H2O,i+1} + \dot{n}_{inert}. \quad (28)$$

The molar fraction of each species was calculated using the equation:

Table 2. *Activation energies and pre-exponential factors for forward and backward WGSR obtained from literature; the rate constants for WGSR were calculated at operating temperature 1073 K*

Source	E_{af} [J/mol]	k_{0f} [(l/mol)$^{0.5}$ s^{-1}]	E_{ab} [J/mol]	k_{0b} [(l/mol)$^{0.5}$ s^{-1}]	k_f [(cm^3/mol)$^{0.5}$ s^{-1}]	k_b [(cm^3/mol)$^{0.5}$ s^{-1}]
Culbertson [8]	334.72	$7.7\cdot10^{45}\cdot T^{-10}$ (i)	/	/	6.10	/
Graven & Long [9]	281.58	$5.0\cdot10^{12}$	238.49	$9.5\cdot10^{10}$	3.10	7.37
Bustamante [10]	253.55	$1.52\cdot10^{10}$	218.40	$6.65\cdot10^{8}$	0.22	0.49
(i)The pre-exponential factor is also temperature dependant therefore the correct unit is K^{10} (l/mol)$^{0.5}$ s^{-1}.						

$$x_{j,i+1} = \frac{\dot{n}_{j,i+1}}{\dot{n}_{R,i+1}}, \tag{29}$$

where j represents individual specie (H_2, CO_2, CO or H_2O).

Similarly, the concentration of each species was calculated:

$$c_{j,i+1} = \frac{\dot{n}_{j,i+1}}{\dot{n}_{R,i+1}} \cdot \frac{p_R}{R \cdot T} = x_{j,i+1} \cdot \frac{p_R}{R \cdot T}, \tag{30}$$

where the pressure on the retentate side was held at constant value p_R = 50 bar. The partial H_2 pressure on the retentate side was calculated as:

$$p_{R\mathrm{H2},i+1} = x_{R\mathrm{H2},i+1} \cdot p_R. \tag{31}$$

In order to calculate heat duty the heat of reaction ΔH_R needs to be calculated. This was done by using the van't Hoff Relation based on source [6]:

$$\Delta H_R = -R \cdot T^2 \cdot \frac{\partial}{\partial T} ln\, K_{eq}(T, p), \tag{32}$$

where the logarithm of equilibrium constant K_{eq} was obtained with the equation reported in Bustamante [10] which was based on the study from Singh and Saraf [7]:

$$ln\, K_{eq} = \frac{1}{1.987} \cdot \begin{pmatrix} \frac{9998.22}{T} - 10.213 + \\ +2.7456 \cdot 10^{-3} \cdot T - \\ -0.453 \cdot 10^{-6} \cdot T^2 - \\ -0.201 \cdot ln\, T \end{pmatrix}. \tag{33}$$

And the CO conversion X_{CO} was deduced as follows:

$$X_{CO,i+1} = \frac{\dot{n}_{CO,in} - \dot{n}_{CO,i+1}}{\dot{n}_{CO,in}}. \tag{34}$$

b) Permeate side:

Similarly as on the retentate side the Law of Conservation of Mass must also apply for each section on the permeate side. The molar flow of H_2 and N_2 mixture was calculated as:

$$\dot{n}_{P,i+1} = \dot{n}_{P,i} - \dot{n}_{\mathrm{H2},i+1}. \tag{35}$$

Because the molar flow of the N_2 sweeping gas is constant throughout the reactor, the molar flow of H_2 on the permeated side can be written as:

$$\dot{n}_{P\mathrm{H2},i+1} = \dot{n}_{P,i+1} - \dot{n}_{\mathrm{N2}}. \tag{36}$$

Samilarly as on the retentate side, the molar fraction of each species was calculated using the Eq.:

$$x_{j,i+1} = \frac{\dot{n}_{j,i+1}}{\dot{n}_{R,i+1}}, \tag{37}$$

where j represents individual specie (H_2 or N_2).

The partial H_2 pressure on the permeate side was calculated as:

$$p_{PH2,i+1} = x_{PH2,i+1} \cdot p_P. \tag{38}$$

where the pressure on the permeate side was held at the constant value p_P = 1 bar.

2.3 Model Design in Aspen Plus

The simulation was performed using the Aspen Plus reactor model unit where chemical reactions of WGS and side reactions (H_2S and COS formation) were modelled. The input data were temperature, pressure, molar flow, composition of syngas and formulas of chemical reactions that take place inside the reactor. The shortcoming of the model was that the program had no information about the kinetics of the WGSR and hence no knowledge of the extent of the CO conversion and the H_2 permeation through the membrane. These two parameters were calculated based on the kinetics of the WGSR and imported from Mathematica (see Fig. 4). That gave us more accurate predictions of the molar flow of H_2 in the permeate stream and the achieved CO conversion

in the WGSMR. Based on these two parameters and the initial and boundary conditions (see subchapter 2.1) the simulation of the WGSMR was performed.

The model of the MR was designed to achieve the isothermal temperature distribution throughout the entire reactor. This is done in such a way that indirect water cooling is applied in a co-current direction to syngas flow. To attain efficient heat removal, the water evaporates almost throughout the entire reactor and gets slightly superheated at the end of the reactor. It is presumed that the WGSR will be most intensive at the beginning of the reactor thus, most of the heat will be released in the first part of the reactor. The sweeping N_2 gas enters the reactor in a counter-current way. The reason for that is to keep the H_2 partial pressure difference reasonably high in all parts of the reactor in order to achieve better flux through the reactor's membrane.

3 RESULTS AND DISCUSSION

3.1 Calculations in Mathematica

In the subchapters bellow the WGSR kinetics are discussed and calculations for the base case model are presented. A sensitivity analysis of the model is made by varying different parameters like the membrane's permeance, length (indirectly the surface area) of the reactor and the molar fraction of H_2 in the permeate stream.

3.1.1 WGSR Kinetics

There is some discrepancy between the uncatalysed WGSR kinetic data available from literature. For this purpose, three different studies were compared all using the Bradford mechanism [4] to describe the WGSR. Table 2 presents activation energies and pre-exponential factors obtained from these studies.

The rate coefficients for forward and backward reaction were calculated according to Eq. (3). As shown in Table 2, the rate coefficients calculated with values obtained from Bustamante [10] are one order smaller than those obtained with values from Graven and Long [9]. Even though Bustamante's research [10] was conducted at elevated pressures (16.21 bar), and Graven and Long's [9] only at atmospheric pressure, the results from Graven and Long's study [9] are in better agreement with Culbertson [8] who conducted his study at even higher pressures and temperatures (196.5 to 496.4 bar and 1200 to 2100 K).

The calculations showed that the reaction rate according to Bustamante [10] is one order smaller than the one predicted from Graven and Long [9] (see Fig. 7). This has also been confirmed in the study from Culbertson [8], therefore the decision was made that the coefficients deduced from Graven and Long [9] will be used in the WGSR kinetic study.

3.1.2 Base Case Studies

One of the purposes of this study was to determine if the permeation through the membrane is sufficient or if there is a build-up of H_2 on the retentate side. First, the comparison was made by using the molar flows of both processes calculated by Eqs. (26) and (27).

Only in the first two sections the reaction rate is slightly faster than the permeation (on Fig.

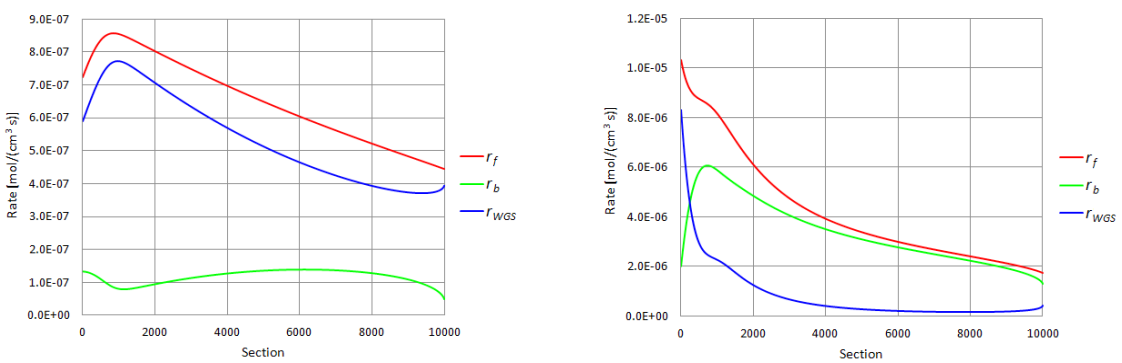

a) *Bustamante's model* b) *Graven & Long's model*

Fig. 7. *Rate of reaction based on different models*

8 the difference is negative) after which the rate of permeation becomes faster than the production of H_2. As seen from Fig. 8, the maximum difference is reached around the 400th section and the permeation rate becomes almost equal to the reaction rate around the 4000th section. The rate of reaction rises slightly at the end because at that point the concentration of H_2 is close to zero and the effect of the backward WGSR almost disappears. The increase in the reaction rate also causes the rate of permeation to increase, because more H_2 is produced, which immediately permeates through the membrane because the process is not permeation limited.

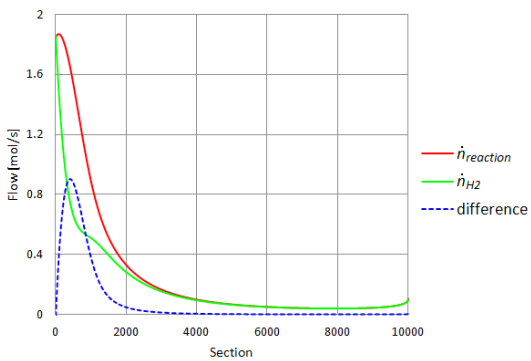

Fig. 8. *Difference between the rate of H_2 production and the rate of H_2 permeation in each section of the reactor*

As it can be seen from Fig. 9, the molar fraction of H_2 actually rises at the beginning even though the rate of permeation is greater as the rate of formation. By constantly extracting H_2 from the retentate stream, the joint molar flow also decreases. Since at the beginning the difference between the permeation and the production rates of H_2 is not big enough, the H_2 molar flow in retentate stream is decreasing but not as fast as the molar flows of H_2O and CO. As a consequence, the molar fraction of H_2 actually rises slightly until the 64th section where, on behalf of a sharp increase in the permeation rate, H_2 starts to rapidly permeate through the membrane.

After reaching the peak at the 64th section the molar fraction of H_2 starts to decrease fast until the 1000th section. Around the 2000th section the permeation already slows down considerably and around the 4000th section most of H_2 present in the retentate stream at the beginning and H_2 converted from CO until that point permeate through the membrane. From that point on, only the H_2 that is converted from CO is permeating through the membrane.

Rapid permeation of H_2 is responsible for molar fractions of H_2O and CO to experience the first inflection point around the 400th section. The fractions reach the second inflection point around 2000th section, where majority of H_2 on the retentate side already permeated through the membrane. From that point on both fractions gradually reduce towards the end of reactor where the consumption of H_2O and CO again slightly increases on behalf of increase in the reaction rate.

The molar fraction of CO_2 is increasing fast in the first 2000 sections because of H_2 permeation and because of CO conversion. This can be seen from a graph where after 2000 sections the rate of CO_2 formation starts to decrease since virtually all of H_2 that was present in the stream permeates through the membrane. At the end, the rate of CO_2 formation slightly increases on behalf of the increase in the reaction rate.

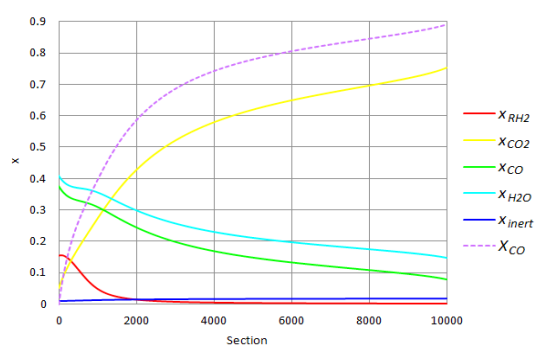

Fig. 9. *Change in molar fractions of species and the CO conversion throughout the reactor*

Based on the input values, the calculated molar composition of the retentate stream is presented in Table 3. Below, these values are also compared to the simulation results from Aspen Plus.

In order to keep the MR operating at isothermal conditions, approximately two thirds of all heat, produced from the WGSR, would need to be removed from the reactor in the first 2000 sections (see Fig. 10). The cooling tubes should be distributed in such a way that they would insure

the reactor to operate at isothermal conditions and to prevent the formation of any hotspots in the reactor.

Table 3. *Input and output values from Mathematica program*

Input values (SYNGAS)					
species	H_2O	CO	H_2	CO_2	inert
x_i	0.410	0.375	0.154	0.052	0.009
Output values (GAS-2)					
species	CO_2	H_2O	CO	inert	H_2
x_i	0.754	0.148	0.080	0.018	$3.0 \cdot 10^{-4}$

It should also be noted that by introducing the cooling tubes into the reactor the CO conversion may suffer minor penalties because the reaction volume for the WGSR will be reduced.

The shape of the curve resembles the curve of the CO conversion, because with more CO converted more heat is released. The calculated cumulative heat duty released from the WGSR is $\dot{Q} = 63.4$ MW.

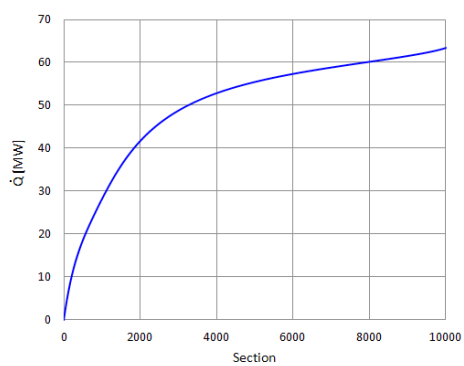

Fig. 10. *Cumulative distribution of heat released in the WGSMR*

3.1.3 Influence of Membrane's Permeance on CO Conversion

The influence of membrane's permeance on the CO conversion was studied using the MR designed for base case studies. The only parameter that was changed was the membrane's permeance. In this analysis the permeance was set to the value $k' = 3 \cdot 10^{-5}$ mol m^{-2} s^{-1} $Pa^{-0.5}$. The calculations show that in the MR with such material permeance the processes would become permeation limited.

The graph in Fig. 11 shows that the reaction rate is faster than the permeation rate in the first 600 sections. Beyond that point permeation is faster but it remains fairly low. At the beginning permeation slightly rises because of the H_2 build-up which increases the H_2 partial pressure and enhances the flux through the membrane. The WGSR proceeds fast in the first 1000 sections and then it remains low through the entire reactor. The blue, dashed line shows the difference between both processes.

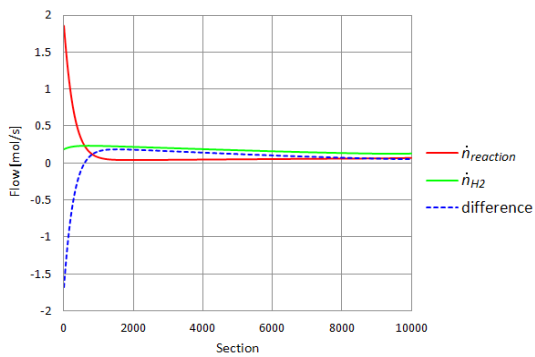

Fig. 11. *Difference between the rate of H_2 production and the rate of H_2 permeation with one order smaller permeance*

The graph in Fig. 12 shows the build-up of H_2 molar fraction in the retentate stream. After the reaction rate becomes steady, the H_2 fraction starts to gradually decrease on behalf of slow permeation. As the permeation is very limited, all of H_2 does not succeed in permeating through the membrane, therefore in the end there is still around 4% of H_2 left in the retentate stream.

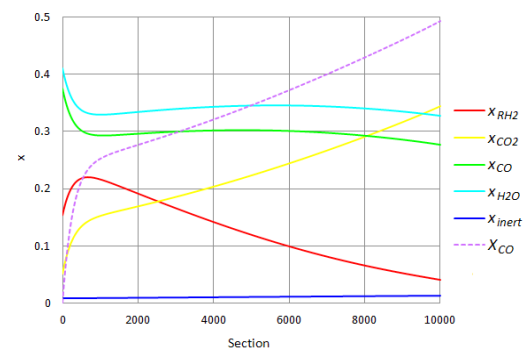

Fig. 12. *Change in molar fractions of species and the CO conversion with one order smaller permeance*

The reactor achieves only 50% CO conversion because the extraction of H_2 is too slow and it does not shift the equilibrium as far to the product side as in the base case scenario.

3.1.4 Influence of Reactor's Surface Area and H_2 Molar Fraction in Permeated Stream on CO Conversion

The influence of the reactor's surface area on CO conversion was studied by varying the length of the reactor. Additionally, the influence of different molar compositions in the permeate stream was studied. By changing both parameters Table 4 was obtained.

The table shows that reducing the molar fraction of H_2 in the permeate stream would favour the CO conversion. This is due to the fact that the partial pressure of H_2 is lower and thus, enhances the flux through the membrane which indirectly affects the CO conversion.

Increasing the reactor's surface, by extending the length of the reactor, also favours the CO conversion. By enlarging the membrane surface area, more H_2 can permeate through, which shifts the WGSR more to the product side, and helps improve the CO conversion.

To further determine the influence of surface area, the reactor with 70 m in length and H_2 molar fraction x_{H2} = 0.45 was simulated. The reactor achieved only 92.3% CO conversion. This shows that extending a reactor further would help achieve better conversions, but from economic point of view investment costs would be enormous to build such a big reactor. As discussed in earlier chapters, it would be better to use the catalyst because the surface area is already large enough and in the latter part of the MR the limiting process is the WGSR rate.

3.2 Simulation Results in Aspen Plus

The model simulated on the basis of the calculations obtained from the Mathematica base case model is presented in the previous subchapter.

Table 4. *CO conversion at different H_2 molar fractions and lengths of reactor*

		L = 30 m			L = 40 m			L = 50 m		
		X_{CO}	$\dot{n}_{N2}$ [mol/s]	$\dot{n}_{P,H2}$ [mol/s]	X_{CO}	$\dot{n}_{N2}$ [mol/s]	$\dot{n}_{P,H2}$ [mol/s]	X_{CO}	$\dot{n}_{N2}$ [mol/s]	$\dot{n}_{P,H2}$ [mol/s]
x_{H2}	0.45	88.0	3281.43	2684.73	90.1	3335.05	2728.57	91.2	3363.35	2751.82
	0.5	87.0	2664.53	2664.49	89.1	2707.63	2707.57	90.2	2730.35	2730.3
	0.55	86.0	2162.35	2642.9	88.0	2196.87	2685.16	89.1	2215.03	2707.32

Table 5. *Molar compositions of gas streams(see Fig. 13)*

Rawgas (on the exit from the gasifier)									
species	CO	H_2	H_2O	CO_2	Ar	H_2S	N_2	COS	HCl
x_i	0.560	0.230	0.120	0.077	$4.8\cdot10^{-3}$	$4.5\cdot10^{-3}$	$4.0\cdot10^{-3}$	$3.9\cdot10^{-4}$	$6.7\cdot10^{-5}$
Syngas (after quench)									
species	H_2O	CO	H_2	CO_2	Ar	H_2S	N_2	COS	HCl
x_i	0.410	0.375	0.154	0.052	$3.2\cdot10^{-3}$	$3.0\cdot10^{-3}$	$2.7\cdot10^{-3}$	$2.6\cdot10^{-4}$	$4.5\cdot10^{-5}$
Gas-2 (retentate stream on the exit of the MR)									
species	CO_2	H_2O	CO	Ar	H_2S	N_2	H_2	COS	HCl
x_i	0.769	0.140	0.072	$6.3\cdot10^{-3}$	$5.9\cdot10^{-3}$	$5.3\cdot10^{-3}$	$5.3\cdot10^{-4}$	$5.2\cdot10^{-4}$	$8.8\cdot10^{-5}$
Gas-3 (after catalytic burner)									
species	CO_2	H_2O	SO_2	Ar	N_2	O_2	CO	H_2	H_2S
x_i	0.835	0.146	$6.4\cdot10^{-3}$	$6.2\cdot10^{-3}$	$5.2\cdot10^{-3}$	$2.0\cdot10^{-3}$	0	0	0
GT-gas (permeate stream on the exit of the MR)									
species	H_2	N_2	CO	H_2O	CO_2	Ar	H_2S	COS	HCl
x_i	0.5	0.5	0	0	0	0	0	0	0

This chapter deals with the influence of absolute pressure on the permeate side as regards to the power demand for compression of H_2/N_2 mixture.

3.2.1 Base Case Studies

The input variables for the simulation in Aspen Plus were the same as the values for model in Mathematica. The only additional data that the model in Aspen needed were the values for CO conversion and the molar flow of permeated H_2. On the basis of the simulation, the molar compositions of gas streams were obtained (see Table 5). The other calculated data are presented in the flowsheet diagram presented in Fig. 13.

The molar fraction of CH_4 was left out of this table because the gasifier model in Aspen Plus predicts that only a small fraction of methane $x_{CH4} = 3.8 \cdot 10^{-5}$ is formed.

The values predicted from the simulation in Aspen Plus and the calculations from Mathematica are in good agreement. In general, the model in Aspen predicts that more CO should be converted for a given CO conversion, because the fractions of CO_2 and H_2 are slightly higher and the fractions of CO and H_2O are slightly smaller as predicted in Mathematica. The calculated heat duty is in very good agreement between both models.

At the exit of the catalytic burner, the temperature of CO_2 rich stream reaches 1200 °C; therefore, there is a great amount of heat available for other processes. A considerable amount of SO_2 present in the stream can be cleaned of sulphur using the conventional Flue gas desulphurisation (FGD) technologies. At this point it should be mentioned that the MR can also be used for direct thermal decomposition of H_2S. Studies on this topic have already been conducted by several authors [12] to [14] and this could be one of the future features integrated in the WGSMR.

3.2.2 Influence of Absolute Pressure on Power Demand for Compression

The influence of the absolute pressure at the permeate side on the power demand for compression of H_2 and N_2 mixture was studied at three different pressures and at constant H_2 molar fraction $x_{H2} = 0.5$.

The change in the absolute pressure on the permeate side effects the H_2 permeation through the membrane because the partial pressure is also changed. As a consequence different H_2 molar flows on the exit of the MR are obtained. To adequately compare the power demand at different operating conditions, the specific work w_{comp} was introduced and defined as:

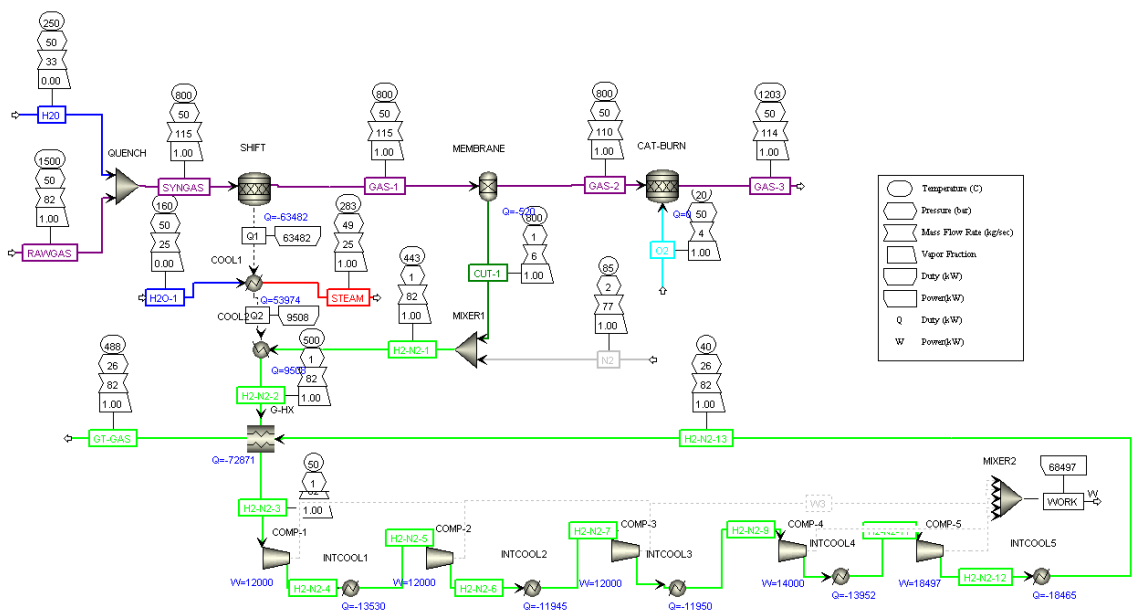

Fig. 13. *Flowsheet diagram used for WGSMR simulations*

$$w_{comp} = \frac{P_{comp}}{\dot{n}_P}, \quad (39)$$

where P_{comp} is the joint power demand of all stages and $\dot{n}_P$ the molar flow of the permeate stream. The calculated data are presented in Table 6.

Table 6. *Comparison of specific work for compression of H_2 to 26 bar*

p [bar]	1	2	3
P_{comp} [MW]	68.497	51.127	45.475
$\dot{n}_P$ [mol/s]	5415.2	5222.2	5075.6
w_{comp} [kJ/mol]	12.65	9.79	8.96

The calculated data show that specific power demand for the base case (1 bar) is relatively high compared to other two cases. In cases of 2 and 3 bar the power demand is not that different; therefore, operating at 2 bar would be an inviting option. In the future, it would be reasonable to study the trade-off between the higher H_2 production and the lower power consumption for compression.

4 CONCLUSIONS

The WGSR kinetics was described with Bradford mechanism [4] together with the kinetic data obtained from Graven and Long's [9] experimental results. The calculations performed in Mathematica were used to calculate the CO conversion and the H_2 flux through the membrane. The calculated data were then imported in Aspen Plus as input (or initial) values for simulations. The model in Aspen Plus was designed as a black box model, simulating the processes based on the initial and boundary conditions and the calculations obtained from Mathematica. The results, derived from both models, are in good agreement with each other and support the correctness of the designed model.

Based on the operational conditions of the designed reactor the membrane material based on Pd was selected. The calculations show that the membrane material with permeance $k' = 3 \cdot 10^{-4}$ mol m^{-2} s^{-1} Pa$^{-0.5}$. would be sufficient for the CO conversion because the process would be reaction and not permeation limited. The CO conversion could be enhanced by increasing the reaction rate with the use of high temperature catalyst or with higher process temperatures. Other studies emphasized that Pd also has some catalytic properties for the WGSR but this was not included in the designed model. However, in the future it would be reasonable to determine the catalytic properties of Pd to accurately predict the WGSR rate, as well. It was established that one order smaller membrane permeance would reduce the CO conversion to 50% because the process would be permeation limited.

Based on the selected boundary conditions the designed model predicts that 89.1% CO conversion can be achieved. With length increase of 75% and H_2 molar fraction of $x_{H2} = 0.45$ in the permeate stream 92.3% conversion was achieved. But from economic point of view the gain in CO conversion would not justify the investment cost for such a big reactor.

Changing the absolute pressure on the permeate side shows that the trade-off between the CO conversion and the power demand for compression of H_2/N_2 gas stream needs to be approached by further research. The specific power demand shows that it would be reasonable to set the absolute pressure to 2 bar.

The retentate stream is fed to the catalytic burner, where the unconverted CO, unpermeated H_2 and H_2S are burned to produce additional heat. Afterwards, the stream contains the SO_2 which can be removed with conventional FGD technologies. Another possibility for the MR in the future may be the thermal decomposition of H_2S. However, in order to incorporate the process into the MR, it needs to be studied further.

In general, the study shows that the WGSMR is feasible, but there are still many issues that need to be addressed. First of all, the membrane material must retain its structural stability and permeability during the operating conditions that are stated. If the material cannot withstand the acid environment, pre-cleaning of syngas would be needed. Proper cooling of the reactor also needs to be designed to avoid hotspots and to keep the reactor operating at isothermal conditions. By introducing cooling tubes into the reactor, the CO conversion may suffer minor penalties because less reaction volume will be available for the WGSR to take place.

5 ACKNOWLEDGEMENT

The authors would like to thank the reviewers for their constructive criticism, which helped to improve the quality and understanding of this article.

6 NOMENCLATURE

General acronyms

ASU	Air Separation Unit
CCS	Carbon Capture and Storage
FGD	Flue Gas Desulphurisation
IGCC	Integrated Gasification Combined Cycle
MR	Membrane Reactor
PSA	Pressure Swing Adsorption
WGS	Water-Gas Shift
WGSR	Water-Gas Shift Reaction
WGSMR	Water-Gas Shift Membrane Reactor

Physical quantities

$2r$	Outer diameter of tubular membrane, [m]
$[A]$	Concentration, [mol/m^3]
^{a}	Partial order of reaction
a	Width and height of MR, [m]
c	Molar concentration, [mol/m^3]
ΔA	Membrane's surface area of infinitesimal section, [m^2]
ΔH_R	Heat of reaction, [J/mol]
ΔV	Volume surrounding infinitesimal section of the membrane, [m^3]
Δx	Length of infinitesimal section, m
E_a	Energy of activation, [J/mol]
E_{ab}	Energy of activation for backward WGSR, [J/mol]
E_{af}	Energy of activation for forward WGSR, [J/mol]
$_i$	index representing the i^{th} section in numerical calculations
$_j$	index representing individual gas specie
J	Flux through membrane, [mol/(m^2 s)]
k	Rate constant, [(cm^3/mol)$^{0.5}$ s^{-1}]
k_b	Rate constant for backward WGSR, [(cm^3/mol)$^{0.5}$ s^{-1}]
k_f	Rate constant for forward WGSR, [(cm^3/mol)$^{0.5}$ s^{-1}]
k_0	Pre-exponential factor, [(l/mol)$^{0.5}$ s^{-1}]
k_{0b}	Pre-exponential factor for backward WGSR, [(l/mol)$^{0.5}$ s^{-1}]
k_{0f}	Pre-exponential factor for forward WGSR, [(l/mol)$^{0.5}$ s^{-1}]
k'	Membrane's permeance, [mol m^{-2} s^{-1} Pa$^{-0.5}$.]
K_{eq}	Equilibrium constant
L	Length of reactor, [m]
$\dot{n}$	Molar flow, [mol/s]
$\dot{n}_R$	Molar flow of retentate gas stream, [mol/s]
$\dot{n}_P$	Molar flow of permeate gas stream, [mol/s]
$\dot{n}_{CO}$	Molar flow of CO, [mol/s]
$\dot{n}_{CO2}$	Molar flow of CO_2, [mol/s]
$\dot{n}_{H2}$	Molar flow of H_2 permeating through membrane, [mol/s]
$\dot{n}_{H2O}$	Molar flow of H_2O, [mol/s]
$\dot{n}_{inert}$	Molar flow of inert gases, [mol/s]
$\dot{n}_{N2}$	Molar flow of N_2 (carrier gas) on permeate side of the membrane, [mol/s]
$\dot{n}_{reaction}$	Molar flow of species produced or consumed during the WGSR, [mol/s]
$\dot{n}_{PH2}$	Molar flow of H_2 on permeate side of the membrane, [mol/s]
$\dot{n}_{RH2}$	Molar flow of H_2 on the retentate side of the membrane, [mol/s]
N_{TUBES}	Number of tubes in MR
p	Pressure, [bar]
p_P	Pressure on permeate side of MR, [bar]
p_{PH2}	Partial pressure of H_2 on permeate side of the membrane, [bar]
p_R	Pressure on retentate side of MR, [bar]
p_{RH2}	Partial pressure of H_2 on retentate side of the membrane, [bar]
P_{comp}	Power demand for H_2 compression, [W]
$\dot{Q}$	Heat duty, [W]
r	Rate of reaction, [mol/(cm^3 s)]
r_b	Rate of reaction for backward WGSR, [mol/(cm^3 s)]
r_f	Rate of reaction for forward WGSR, [mol/(cm^3 s)]
R	Universal gas constant, [J/(mol K)]
T	Temperature, [K]
w_{comp}	Specific work for H_2 compression, [J/mol]
x	Molar composition or molar fraction
x_{RH2}	Molar fraction of H_2 on retentate side of the membrane
x_{PH2}	Molar fraction of H_2 on permeate side of the membrane
X_{CO}	CO conversion

7 REFERENCES

[1] Donaldson, A.M., Mukherjee, K.K. (2006). Gas turbine "refueling" via IGCC POWER Magazine, from: *http://www.powermag.com/gas/Gas-turbine-&quotrefueling%22-via-IGCC_540_p3.html,* accesed on 2009-06-14.

[2] Ladebeck, J.R., Wagner, J.P. (2003). Catalyst development for water-gas shift. *Handbook of Fuel Cells - Fundamentals, Technology and Applications*, vol. 3, part 2, p. 190-201.

[3] Killmeyer, R., Rothenberger, K., Howard, B., Ciocco, M., Morreale, B., Enick, R., Bustamante, F. (2003). *Water-gas shift membrane reactor studies*. US DOE, NETL, Berkeley.

[4] Bradford, B.W. (1933). The water-gas reaction in low-pressure explosions. *Journal of the Chemical Society*, p. 1557-1563, DOI 10.1039/jr9330001557.

[5] Ciocco, M.V., Iyoha, O., Enick, R.M., Killmeyer, R.P. (2007). *High-temperature water-gas shift membrane study*. NETL, South Park.

[6] Lebon, G., Jou, D., Casas-Vazquez, J. (2008). *Understanding Non-equilibrium Thermodynamics: Foundations, Applications, Frontiers*. Springer-Verlag, Berlin, DOI: 10.1007/978-3-540-74252-4.

[7] Singh, C.P., Saraf, D.N. (1977). Simulation of high-temperature water-gas shift reactors. *Industrial and Engineering Process Design and Development*, vol. 16, no. 3, p. 313-319, DOI:10.1021/i260063a012.

[8] Culbertson, B., Sivaramakrishnan, R., Brezinsky, K. (2008). Elevated pressure thermal experiments and modeling studies on the water-gas shift reaction. *Journal of Propulsion and Power*, vol. 24, no. 5, p. 1085-1092, DOI:10.2514/1.31897.

[9] Graven, W.M., Long, J.F. (1954). Kinetics and mechanisms of the two opposing reactions of equilibrium $CO + H_2O = CO_2 + H_2$. *Journal of the American Chemical Society*, vol. 76, p. 2602-2607, DOI:10.1021/ja01639a002.

[10] Bustamante-Londono, F. (2004). *The high-temperature, high-pressure homogeneous water-gas shift reaction in a membrane reactor.* Ph.D. Thesis, University of Pittsburgh, Pittsburgh.

[11] Enick, R., Bustamante, F., Iyoha, O., Howard, B., Killmeyer, R., Morreale, B., Ciocco, M. (2004). *Conducting the homogeneous water-gas shift reaction in a palladium/copper alloy membrane reactor at high temperature and pressure*. NETL, Pittsburgh.

[12] Edlund, D. (1996). *A membrane reactor for H_2S decomposition*. Bend Research, Inc., Morgantown.

[13] Ma, Y. H., Moser, W.R., Pien, S., Shelekhin, A.B. (1994). *Development of hollow fiber catalytic membrane reactors for high temperature gas cleanup*. Worcester Polytechnic Institute, Worcester.

[14] US 7,163,670 B2 - Patent, Agarwal, P.K., Ackerman, J. (2007). *Membrane for Hydrogen Recovery from Streams Containing Hydrogen Sulfide*, University of Wyoming, Wyoming.